# Testing the performance of a recent radon-hazard evaluation in the municipality of Gran, eastern Norway

**Mark A. Smethurst[1], Aud Venke Sundal[2], Terje Strand[3] and Bernard Bingen[1]**

*[1] Geological Survey of Norway (NGU), 7491 Trondheim, Norway.*
*[2]Institute of Geography, University of Edinburgh, Drummond Street, Edinburgh EH8 9XP, UK.*
*[3]Department of Physics, University of Oslo, P.O. Box 1048 Blindern, 0316 Oslo, Norway.*
*E-mail:mark.smethurst@ngu.no*

The Geological Survey of Norway and Norwegian Radiation Protection Authority have produced a new overview of radon hazard in the most densely populated part of Norway around the capital city, Oslo, and Oslofjord. We look closely at the performance of the radon-hazard evaluation within a rectangular area 520 km$^2$ in size centred on the municipality of Gran. The uranium-rich alum shale and superficial deposits associated with it are the principal sources of radon in the area. Small, isolated granite bodies and local, high-permeability glaciofluvial deposits are likely to contribute to elevated radon-hazard levels. The multidisciplinary hazard evaluation is based on direct measurements of radon in indoor air, bedrock geology, drift geology, and radon-daughter (bismuth) mapping using helicopter-borne instruments. Our testing of the hazard evaluation shows that combining signs of radon hazard from each of the data sets in the Gran region produces a liberal hazard map that encloses most of the known areas of severe radon contamination in dwellings, and reveals additional uninhabited areas where similar levels of contamination can be expected if those areas are taken into use for residential purposes without mitigating action. The hazard evaluation in the Gran area is 80.7% efficient in enclosing high indoor radon measurements in the high-hazard zone when this zone occupies 50% of the total geographic area. The probability of this distribution happening by chance is 0.054%. If the hazard prediction bore no relation to the actual distribution of high indoor radon measurements, the efficiency would be around 50%. The radon-hazard evaluation works well over the alum shale and should be used to improve the efficiency of indoor radon mapping programmes and develop strategies for the implementation of radon mitigation measures.

Smethurst, M.A., Sundal, A.V., Strand, T. and Bingen, B. (2008) Testing the performance of a recent radon-hazard evaluation in the municipality of Gran, eastern Norway. *In* Slagstad, T. (ed.) *Geology for Society*, Geological Survey of Norway Special Publication, **11**, pp. 145–154.

## Introduction

In Norway, long-term exposure to radon and its progenies are responsible for 14% of the new cases of lung cancer each year. This corresponds to nearly 300 cases per year. Given the generally poor prognosis for lung cancer, radon is likely to be responsible for as many deaths each year as occur on the roads of Norway. Furthermore, exposure to radon gas in the Norwegian population is increasing due to changes in the way we build houses and how we use the spaces within them (Strand et al. 2001, Strand et al. 2003).

Investigations have shown that the building substrate is the dominant source of radon in Norwegian dwellings (Stranden 1986). The geology of the area around Oslo is complex (Lutro and Nordgulen 2004), characterised by sharp transitions from uranium-rich rock types like alum shale and granite—traditionally associated with hazardous levels of radon in indoor air—to uranium-poor rock types like the majority of sedimentary rocks and mafic igneous rocks. The geological complexity is increased by the presence of superficial deposits that vary widely in permeability from impermeable marine clay to highly permeable glaciofluvial sand and gravel. Permeability is a vital factor governing the transport of radon gas in the ground (Arvela et al. 1994, Sundal et al. 2004). The fact that geological factors influencing the production and transportation of radon gas vary dramatically in and around the capital city, dictates a need in society for geological information that can help identify the areas most likely to be affected by radon.


*Figure 1. The area around Oslofjord evaluated for radon hazard by Smethurst et al. (2006) is outlined in blue (also see Smethurst et al. submitted). The size and shape of this area is governed by the availability of airborne geophysical surveys in the region—one of the data sets used in the evaluation of radon hazard. We look in detail at the performance of the hazard evaluation within the rectangular area marked in black around Gran in the northern part of the region. The field of view in the figure is approximately 140 x 200 km.*

Smethurst et al. (2006) (also see Smethurst et al. submitted) assembled geological information for the area around Oslo and Oslofjord and interpreted it in terms of potential radon hazard as part of the Geological Survey of Norway's recent *geology in the Oslo region* (GEOS) initiative (Figure 1). Naturally, the Norwegian Radiation Protection Authority was an active participant in this part of the GEOS initiative. The data sets were (1) directly measured radon concentrations in indoor air (Strand et al. 2001, 2003), (2) digital bedrock geology (Lutro and Nordgulen 2004), (3) digital drift geology (Geological Survey of Norway), and (4) uranium concentrations in the ground from airborne geophysical surveying (Håbrekke 1982, Beard and Rønning 1997, Beard 1998, 1999, Mogaard 1998, 2001, Mogaard and Beard 2000, Beard and Mogaard 2001, Fugro 2003). Smethurst et al. (2006) interpreted each of them in terms of moderate and high radon hazard (Figure 2) and united these into a single hazard map (Figure 3). This is the map we will be testing in the present contribution.

We choose to test the hazard map in the Gran area marked by the black rectangle in Figure 1. We choose this area because it includes dramatic local variation in radon-hazard levels and is comparatively well covered by measurements of radon in indoor air. There are 549 measurements in all (Figure 4): 22% over 200 Bq $m^{-3}$, 10% over 400 Bq $m^{-3}$ and 3.5% over 1000 Bq $m^{-3}$. The action level in Norway is 200 Bq $m^{-3}$ (NRPA 2000).

## Radon in indoor air

Annual average radon concentrations in indoor air (Strand et al. 2001, 2003) are unevenly distributed across the Gran area (Figure 4), reflecting the uneven distribution of dwellings and known locations of radon hot-spots. The colours of the symbols in Figure 4 clearly show that there are rapid transitions between areas where almost all measurements are over the action level and areas where almost all measurements are below it. Certainly within the tract Brandbu–Jaren–Gran, there are sufficient indoor measurements to create a good picture of radon-hazard hot-spots—without calling upon other data sets. The pattern between these towns and Jevnaker is less clear. There are no geo-referenced data around Grua so any potential radon hazards in this area remain undetected through this data set. The hazard evaluation scheme of Smethurst et al. (submitted) assigns high radon hazard to areas where 20% or more of the indoor radon measurements exceed the action level (Figure 2a).

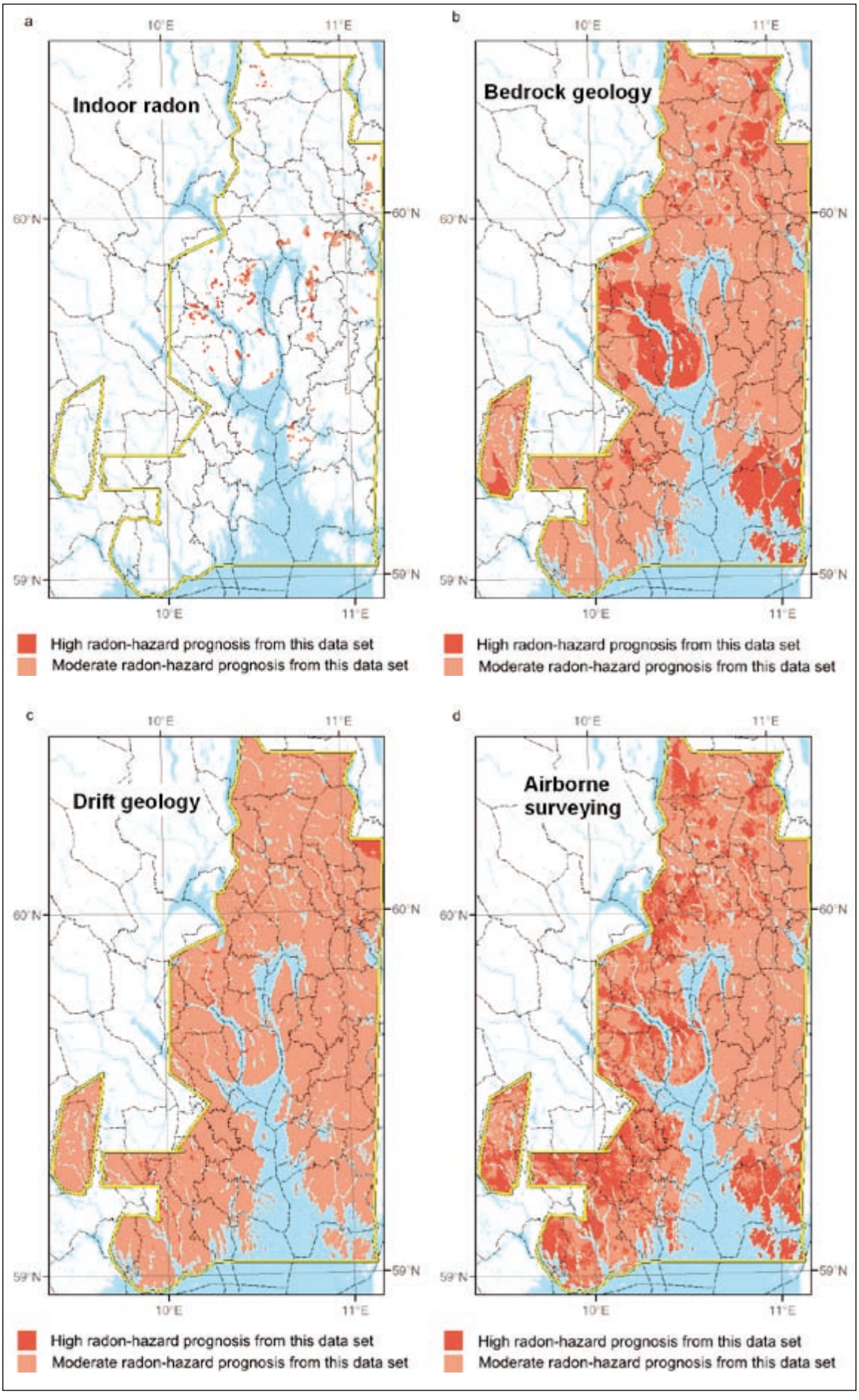


*Figure 2. The radon-hazard prognosis of Smethurst et al. (2006) is based upon four data sets. (a) Areas where 20% or more of the indoor radon-concentration measurements exceed 200 Bq m$^{-3}$ (search radius 300 m, n ≥ 9) are assigned high radon hazard. (b) Alum shale, granite and rhyolite are commonly rich in uranium and areas occupied by these rock types are designated high radon hazard. (c) Highly permeable superficial deposits, in this case largely glaciofluvial deposits, are assigned high radon hazard. (d) Uranium concentrations in the ground from airborne gamma-ray spectrometer surveying. Areas where uranium concentrations exceed 4 ppm are designated high radon hazard. The hazard prognoses from these four data sets are combined into the overall hazard map of Figure 3.*

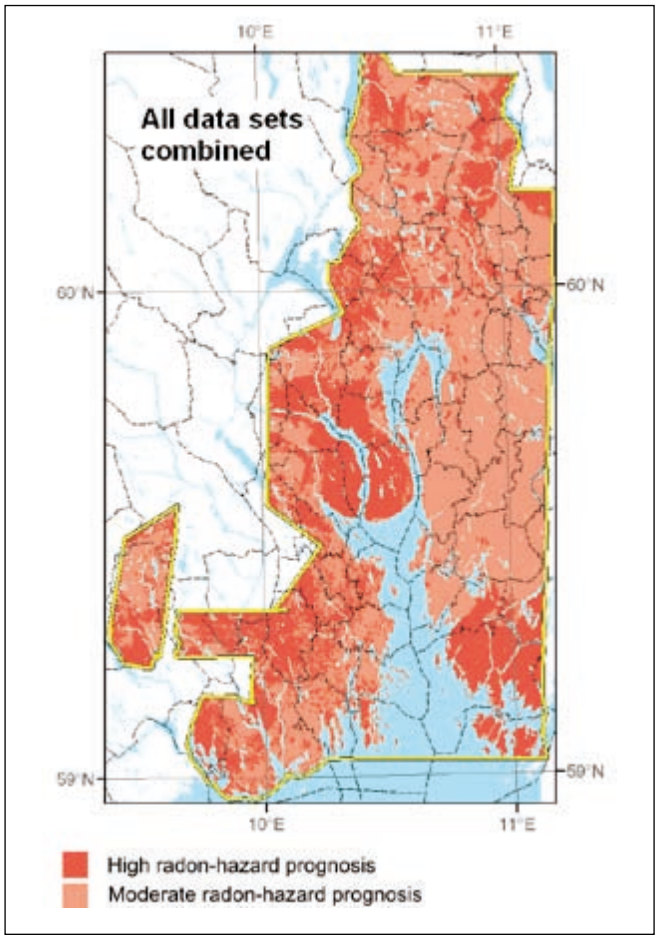


*Figure 3. Large-scale radon-hazard evaluation from the study of Smethurst et al. (2006) (sum of the four maps in Figure 2). This map is now available on the Internet in the form of an interactive map service at http://www.ngu.no/kart/arealis/. (In Norwegian—select the map theme 'Radon aktsomhet'.)*

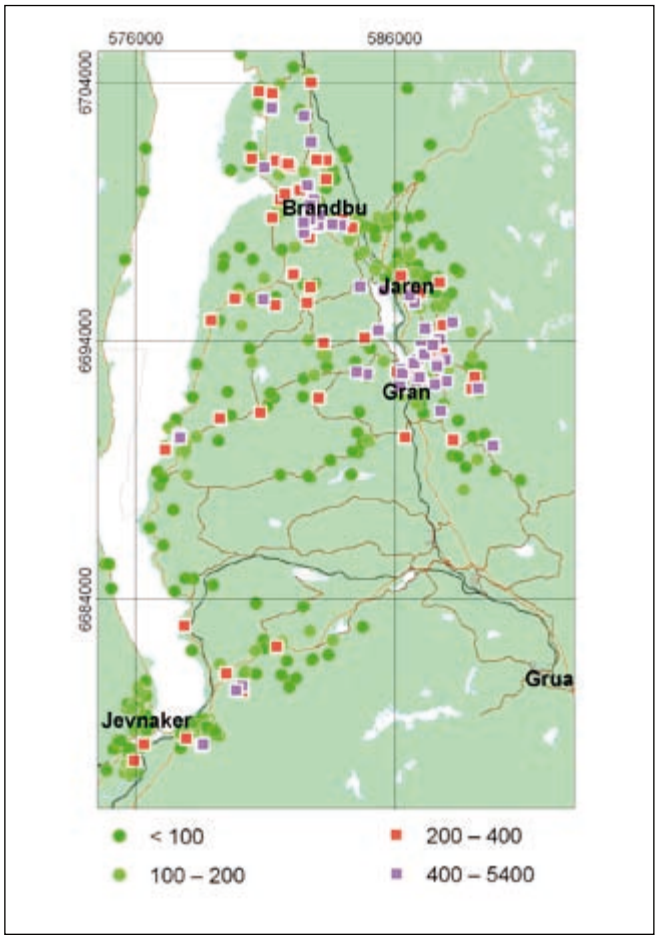


*Figure 4. Radon concentrations in indoor air (Bq $m^{-3}$) for 549 dwellings in the Gran area. Squares denote radon concentrations equal to or above the action level of 200 Bq $m^{-3}$. Data provided by the Norwegian Radiation Protection Authority, Østerås (Strand et al. 2001, 2003). The measured grid is according to datum WGS1984, projection UTM (zone 32N). The Gran study area (field of view) measures 18 x 29 km.*

## Bedrock geology

The bedrock geology around Gran, compiled by Lutro and Nordgulen (2004) and simplified by us, is shown in Figure 5. It is well known that the radon problem area around Brandbu–Jaren–Gran is due to the presence of alum shale in the near surface of the ground. Given that knowledge of the presence of alum shale is sufficient in itself to classify an area as potentially hazardous, the outcrop of the alum shale is classified as a 'high' radon-hazard area (Figure 2b). Figure 5 shows that the radon hot-spots, evident through the mapping of radon in indoor air, are enclosed by the outline of the alum shale. It also demonstrates that there are well-defined areas of alum shale that are not delineated by indoor measurements of radon, either because measurements have not been made in dwellings there, or because there are, as yet, no dwellings in those areas.

The rock types listed on the left-hand side of the legend are known to regularly contain sufficient quantities of uranium to result in a significant radon hazard. Smethurst et al. (submitted) show that 46% of the 1169 indoor radon measurements made in dwellings on granite and rhyolite in the Oslo–Oslofjord area exceed the action level. The areas underlain by these rock types are also classified as high radon hazard (Figure 2b). The bedrock geology map in Figure 5 provides important information on likely sources of radon hazards that are not evident in the indoor radon data set. A notable example is the granite body at Grua, outside the coverage of indoor measurements. Clearly, then, the indoor measurements and bedrock geology complement each other and, together, contribute to a sound hazard evaluation and foundation for follow-up work.

## Superficial deposits

At first glance, a surprisingly large proportion of the radon measurements made in dwellings underlain by sedimentary rocks west of Brandbu–Jaren–Gran are high (Figure 6). This illustrates the importance of considering superficial deposits in radon-hazard evaluation. The superficial deposits symbolised as 'moderate permeability' in Figure 6 are locally derived and con-

tain material from the alum shale. High radon measurements west of Brandbu–Jaren–Gran may be due to smaller outcrops of alum shale (not in Figure 5) and superficial deposits containing alum shale. In their evaluation of radon hazard, Smethurst et al. (submitted) rated high permeability glaciofluvial sands and gravels as high radon hazard (Figure 2c). Intensive measurement of indoor radon concentrations in dwellings built on such deposits at Jevnaker, show that in this case the only high indoor radon measurements were made where the deposits overlie the alum shale (compare Figures 5 and 6).

## Uranium concentration in the near-surface ground from airborne geophysical surveying

Airborne gamma-ray spectrometry detects the decay of radon daughters in the upper 30 to 40 cm of the ground (Otton et al. 1995, Sundevall 2003). Converted to equivalent uranium concentrations, these data are shown in Figure 7 using a simple 3-division colour scale. There is an obvious correlation between uranium concentrations and the incidence of elevated radon concentrations in indoor air. Smethurst et al. (2006) noticed this when examining data for the whole of the Oslo–Oslofjord area and suggested that uranium concentrations of around 4


*Figure 6. Extract from the 1:50,000-scale drift geology map of Kjærnes (1982), simplified to differentiate between deposits with different permeabilities by Bjørn Bergstrøm of the Geological Survey of Norway.*

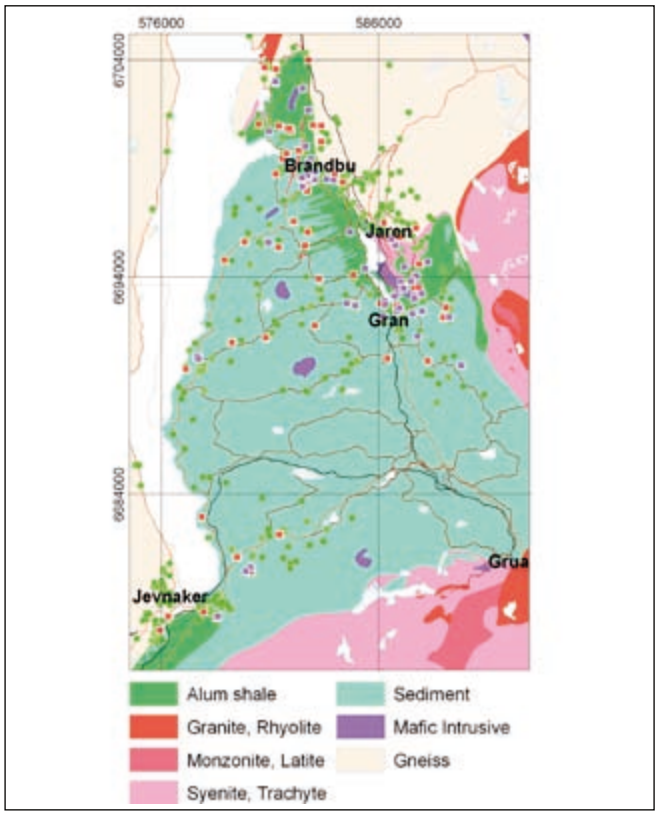


*Figure 5. Extract from the 1:250,000-scale bedrock geology map compiled by Lutro and Nordgulen (2004) for the Oslo Rift and surrounding areas. Original rock-type assignments are merged by us into the broader groups shown. 'Sediment' includes all sedimentary rock types except for alum shale and unconsolidated deposits.*

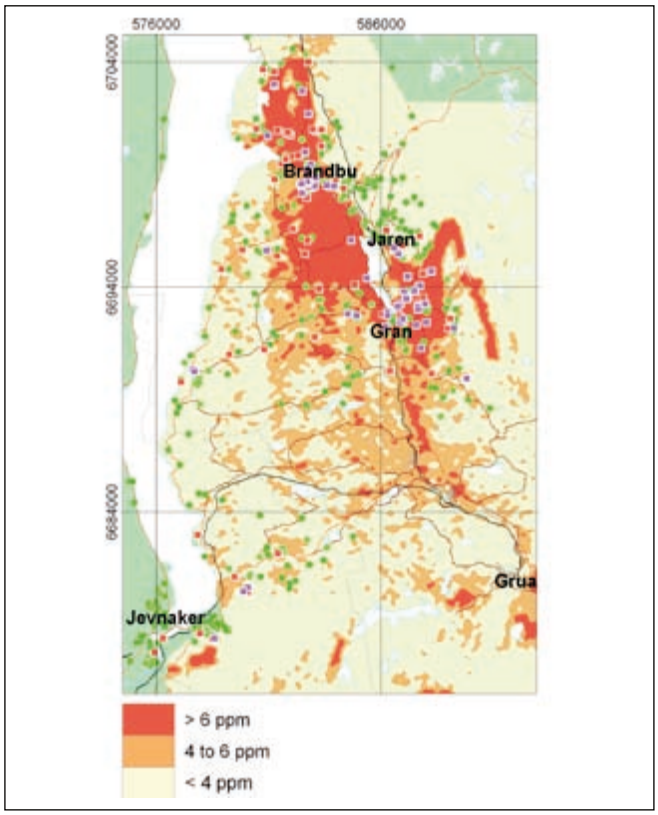


*Figure 7. Uranium concentrations in the near surface of the ground (ppm) based on airborne gamma-ray spectrometer surveys carried out by the Geological Survey of Norway (Beard 1998, Beard and Mogaard 2001). Indoor radon measurements are from Figure 4.*

ppm and above correspond to rates of occurrence of high radon concentrations in indoor air of 20% or more (high = 200 Bq $m^{-3}$ or more). This led them to classify areas with uranium concentrations of 4 ppm or more as high radon hazard (Figure 2d). This corresponds to the brown and red part of Figure 7.

Addition of the uranium data set in the hazard evaluation of the Gran area very significantly complements the three hazard criteria presented above. The data set confirms and refines our knowledge of the position of the alum shale, including the smaller outcrop near Jevnaker. It indicates significant levels of radon in the superficial deposits above sediments west of Brandbu–Jaren–Gran, and clearly shows that the granite bodies around Grua have high uranium contents.

Before moving on to sum up the combined performance of all four hazard criteria in the Gran area, we test the performance of the uranium map alone as a proxy for radon-hazard level. Using the apparent correlation between uranium concentrations and the incidence of elevated radon concentrations in indoor air of Smethurst et al. (2006), we generate the hazard-prediction map in Figure 8. Figure 8 shows the spatial variation in frequency of occurrence of high radon concentrations predicted by the model of Smethurst et al. (2006). Table 1 shows how well this prediction compares with the actual distribution of elevated radon concentrations in indoor air in the 402 measured dwellings on the uranium map. The prediction is sound and we conclude that the setting of a high radon-hazard threshold at 4 ppm uranium (Figure 7) works well in the Gran region. This threshold is equivalent to 20% in Figure 8.

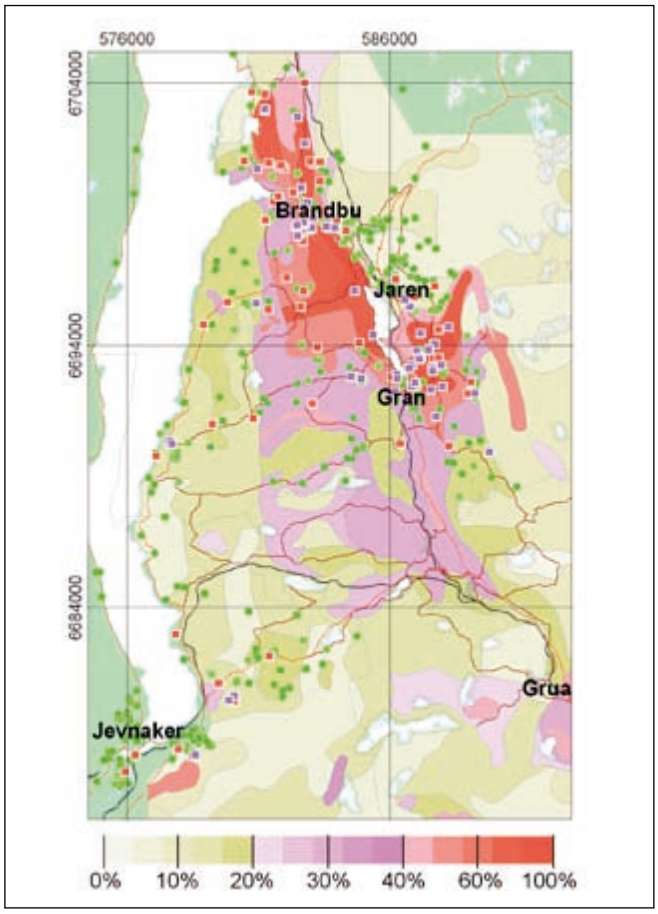


*Figure 8. Radon-hazard interpretation based on the relationship reported by Smethurst et al. (2006) between uranium concentrations in the ground and the percentages of indoor radon measurements above 200 Bq $m^{-3}$. The relationship, based on data throughout the Oslofjord area (Figure 1), is here applied to uranium concentrations in the Gran area. The actual uranium map in Figure 7 is here simplified for clarity and average uranium concentrations within the resulting polygonal areas are converted to* estimates *of the percentages of dwellings with radon levels above 200 Bq $m^{-3}$. The locations of actual indoor measurements are indicated by small, black dots.*

## Summary hazard evaluation in the Gran area

Assembling all of the hazard criteria discussed in the last four sections we arrive at the hazard model in Figure 9a. Straightforward visual inspection of Figure 9a suggests to us that the prediction of elevated hazard conforms well to the actual observations of radon in dwellings in the Gran area. Some conformity is inevitable since clusters of high indoor radon measurements are an integral part of the hazard evaluation (Figure 2a). In the Gran region, though, one can remove this element in the hazard evaluation very easily because high-hazard

*Table 1. The percentages of dwellings with radon concentrations above the action level* predicted *from airborne gamma-ray spectrometer measurements (Figure 8) compared with the* actual *percentages of dwellings with indoor radon concentrations above the action level.*

| Predicted percentage of dwellings with radon concentrations over 200 Bq $m^{-3}$ | Actual percentage of dwellings with radon concentrations over 200 Bq $m^{-3}$ | Prediction correct | Number of dwellings with indoor measurements | Number of measurements over 200 Bq $m^{-3}$ | Maximum radon concentration Bq $m^{-3}$ |
|---|---|---|---|---|---|
| 0%–10% | 3.6% | YES | 56 | 2 | 231 |
| 10%–20% | 18.0% | YES | 161 | 29 | 832 |
| 20%–30% | 15.8% | NO | 19 | 3 | 3134 |
| 30%–40% | 24.5% | NO | 53 | 13 | 1143 |
| 40%–60% | 41.4% | YES | 58 | 24 | 2001 |
| 60%–80% | 80.0% | YES | 35 | 28 | 2330 |
| 80%–100% | 80.0% | YES | 20 | 16 | 5400 |
| Total | | | 402 | 115 | |

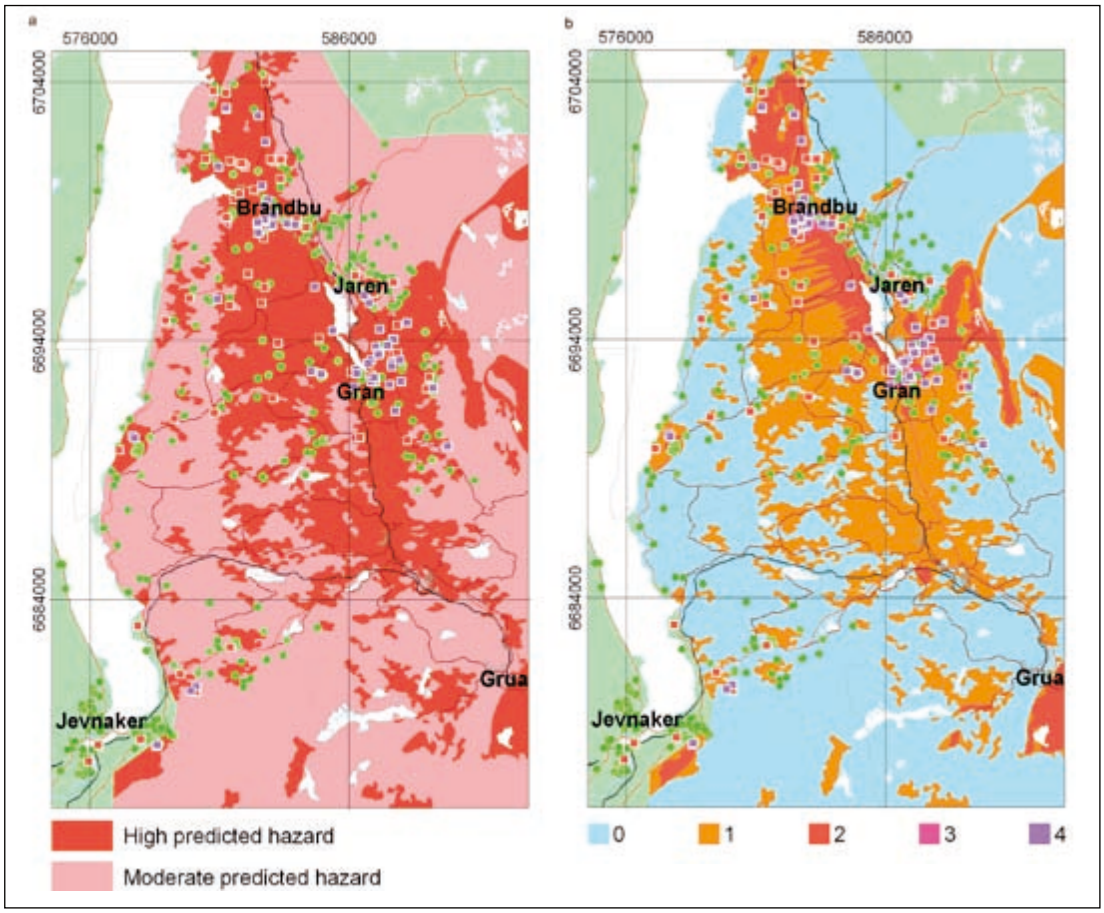


*Figure 9. (a) Overall prediction of radon-hazard levels based on the four factors in Figures 4–7. (b) Number of factors suggesting elevated radon hazard.*

conditions dictated by the indoor measurements are local to Brandbu and Gran that are both already tagged as high hazard by two other independent data sets. Removing the contribution of indoor measurements from the hazard evaluation (Figure 9a) to facilitate an objective test of the hazard map using measurements of radon indoors does not make any difference to the outcome in the Gran area.

A useful byproduct of this approach to radon-hazard evaluation is shown in Figure 9b. The number of different criteria that indicate high radon-hazard level at any given place can be a measure of how sure we are in the assignment of a hazard level. Of course, real life is not that simple and there will always be room for a more considered evaluation of the reliability of hazard-level assignments. The approach to locating areas of elevated radon-hazard level is a generously inclusive one, leading to the definition of large areas with high, predicted radon hazard. This could be described as a 'better to be safe than sorry' approach.

It is interesting at this point to test how efficient the hazard map in Figure 9 is at enveloping high indoor radon measurements within its high radon-hazard zone. Table 2 shows that 41.5% of the indoor measurements in the high-hazard zone are high (≥ 200 Bq $m^{-3}$) while 9.9% in the moderate-hazard zone are high.

We want to go further and establish what proportion of *all* high indoor measurements fall within the high-hazard zone.

*Table 2. The incidence of 'high' (≥ 200 Bq $m^{-3}$) and 'low' (< 200 Bq $m^{-3}$) indoor radon-concentration measurements in what we have designated high- and moderate-hazard regions around Gran (Figure 9a).*

| Hazard assignment | Percentage of dwellings with radon concentrations over 200 Bq $m^{-3}$ | Number of dwellings with indoor measurements | Number of measurements over 200 Bq $m^{-3}$ |
|---|---|---|---|
| High | 41.5% | 241 | 100 |
| Moderate | 9.9% | 152 | 15 |
| Total | | 393 | 115 |

For the result to have any significance we need to adjust for any bias there may be in the spatial densities of indoor radon measurements between the two hazard zones, and for the different sizes of the hazard zones (Table 3).

We do this in a simplistic way in Table 4 by adjusting down the number of observations in the high-hazard zone to equalise sampling densities in the two zones and adjusting down the number of observations of high radon in the moderate-hazard zone to equalise the geographic areas occupied by the hazard zones.

After adjustment, 80.7% of high indoor radon values lie in the area designated as high hazard. The probability of this distribution occurring by chance is 0.000543, or 0.054%.

*Table 3. Sampling bias in the indoor radon-concentration data set. The spatial density of radon measurements in the area designated as high hazard is almost three times that in the area designated moderate hazard. Furthermore, the moderate-hazard area is almost twice as large as the high-hazard area.*

| Hazard assignment | Radon observations per km$^2$ | Area (km$^2$) |
|---|---|---|
| High | 1.73 | 139.6 |
| Moderate | 0.60 | 253.0 |
| Total | | 392.6 |

So, after adjustment for bias and assuming that high- and moderate-hazard zones have the same size, one might expect to find around 80% of the dwellings with high indoor radon concentrations if one were to target dwellings located within the high-hazard zone.

This is effective, but we do not suggest that dwellings in the moderate-hazard zone be ignored. The hazard assessment is based on potentially flawed data of variable quality from place to place and on data that have a limited spatial resolution. Looking beyond the Gran area, it is quite certain that a large number of smaller areas with strong radon contamination and probably some larger areas too, will fall within broad tracts categorised as moderate hazard.

## Consideration of local conditions is important

The hazard assessment works well around Gran. To balance our evaluation of the technique, we show how the usefulness of one of the data sets used in the evaluation can be compromised. Airborne geophysical surveying over Oslo produced a uranium map that was converted into a prediction of radon hazard in a manner similar to that used to generate Figure 8. The result is shown in Figure 10. The airborne surveying correctly highlights alum shale cropping out in the park at Tøyen (right) that, as would be expected, has caused elevated radon concentrations inside some of the buildings in the museum area. The anthropogenic layer covering much of the inner city prevents radiation from the alum shale reaching the airborne measuring system, explaining the abrupt drop in the signal from the alum shale away from the park. The likely complex distribution of the alum shale beneath

*Table 4. The incidence of 'high' (≥ 200 Bq m$^{-3}$) and 'low' (< 200 Bq m$^{-3}$) indoor radon-concentration measurements in high- and moderate-hazard regions adjusted for sampling bias (Table 3 left). Values are also adjusted as if the high- and moderate-hazard regions have the same size (Table 3 right).*

| Hazard assignment | Original number of radon measurements | Original number of measurements over 200 Bq m$^{-3}$ | Adjusted number of radon measurements | Adjusted number of radon measurements over 200 Bq m$^{-3}$ |
|---|---|---|---|---|
| High | 241 | 100 | 83.9 | 34.8 |
| Moderate | 152 | 15 | 83.9 | 8.3 |
| Total | 393 | 115 | 167.8 | 43.1 |

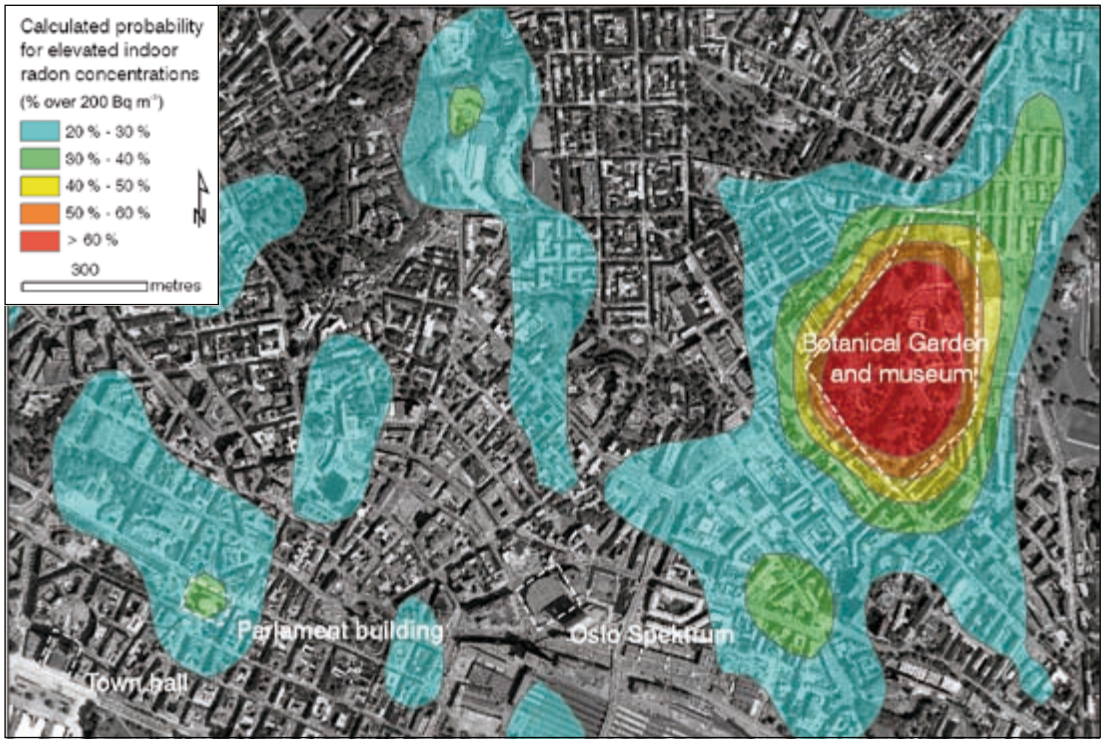


*Figure 10. Radon-hazard model for central Oslo based on airborne measurements alone. The methodology used here is akin to that used in Figure 8 for the Gran area. The approach works rather well at Gran, but in Oslo the uranium-rich alum shale is hidden from the airborne detector by a low permeability, anthropogenic covering. Gamma rays from radon daughter bismuth shine out from openings in the cover, most notably over the parkland around the natural history museum (this Figure). Field of view is 2.6 x 1.6 km.*

Oslo is only partially revealed by the airborne data—in areas of open ground. Nevertheless, the adoption of a multi-data set approach to the hazard evaluation in Oslo means that knowledge of the distribution of rock types and superficial deposits beneath the city is not as compromised as the airborne data set, and radon measurements in Oslo dwellings are just as valuable a source of information as measurements anywhere else.

## Conclusion

The Geological Survey of Norway and Norwegian Radiation Protection Authority recently reported a multi-disciplinary radon-hazard evaluation for the Oslo–Oslofjord region of eastern Norway (Smethurst et al. 2006; static hazard maps are available for download from http://www.ngu.no/ and an interactive map is published on the Norwegian AREALIS environmental map-theme resource at http://www.ngu.no/kart/arealis/). The evaluation is founded upon (1) measurements of radon concentration in indoor air (2) knowledge of bedrock geology, (3) knowledge of drift geology, and (4) measurements of uranium concentration in the ground from airborne geophysical surveying. The hazard evaluation is intended for use at the large scale and cannot be used to evaluate radon hazards on the scale of individual dwellings or even local housing communities.

We test this hazard evaluation in a 520 $km^2$ rectangular area centred on the community of Gran, 40 km north-northwest of Oslo. The uranium-rich alum shale and uranium-rich granite bodies crop out within the test area and indoor radon concentrations reach as much as 25 times the action level. We find that the hazard evaluation describes the distribution of known radon hot-spots well. 41.5% of the indoor radon measurements in the high-hazard areas are above the action level (200 Bq $m^{-3}$) while 9.9% of the measurements in the moderate-hazard areas lie above the action level.

Examining the distribution of high indoor radon concentrations between the high- and moderate-hazard areas, we take account of the different spatial densities of indoor measurements falling in the two hazard categories and apportion high radon measurements between the categories as if the areas occupied by the high and moderate categories were equal. This done, we find that if the high- and moderate-hazard areas were the same size in the Gran area and were sampled equally densely with indoor radon measurements, we would expect 80.7% of all high radon measurements to lie in the high radon-hazard area. In other words, we would expect efficiency in encompassing high-radon dwellings of 80.7%. The probability of this distribution occurring by chance is 0.000543, or 0.054%.

The outcome of this examination, then, is that the radon-hazard mapping of Smethurst et al (2006), later further documented by Smethurst et al. (submitted), works very well in the Gran area by describing known patterns of radon contamination and identifying additional potential radon hazards not yet confirmed by indoor radon measurements.

## Acknowledgements

Tor Erik Finne and John F. Dehls are thanked for their valuable participation in the Geological Survey of Norway's RiO project (radon in the Oslo region). We also thank Sverre Iversen, also of the Survey, for his contribution in publishing the radon-hazard evaluation on the Internet in the form of an interactive map (http://www.ngu.no/kart/arealis/). Gudmund Løvø of the Survey's information department has served the RiO project extremely well by bringing many of the findings of the project to the attention of the Norwegian public in a very lucid manner. Jon Miles and an anonymous reviewer are thanked for critical comments that helped improve the paper.

## References

Arvela, H., Voutilainen, A., Honkamaa, T. and Rosenberg, A. (1994) High indoor radon variations and the thermal behaviour of eskers. *Health Physics*, **67**, 254–260.

Beard, L.P. (1998) Data acquisition and processing—helicopter geophysical survey, Oppkuven and Gran, 1997. *NGU Report 1998.079*, 20 pp.

Beard, L.P. (1999) Data acquisition and processing—helicopter geophysical survey, Larvik, 1998. *NGU Report 1999.026*, 13 pp.

Beard, L.P. and Mogaard, J.O. (2001) Data acquisition and processing—helicopter geophysical survey, Hurdal, 2000. *NGU Report 2001.018*, 16 pp.

Beard, L.P. and Rønning, S. (1997) Data acquisition and processing—helicopter geophysical survey, Krokskogen. *NGU Report 1997.134*, 9 pp.

Fugro Airborne Surveys Central Region (2003) Logistics report, fixed wing borne magnetic, radiometric and VLF–EM survey in the Oslo region, southern Norway. *Fugro Airborne Surveys Report FCR 2241*.

Håbrekke, H. (1982) Magnetic, electromagnetic, VLF and radiometric measurements from helicopter over an area west of Tønsberg in Vestfold and Telemark counties. *NGU Report 1835*, 13 pp. (in Norwegian).

Kjærnes, P.A. (1982) Gran, Quaternary geology map 1815 I, scale 1:50,000, *Norges geologiske undersøkelse*.

Lutro, O. and Nordgulen, Ø. (2004) Oslo Rift, bedrock geology map, scale 1:250,000, *Norges geologiske undersøkelse*.

Mogaard, J.O. (1998) Helicopter-borne geophysical measurements around Larvik, Vestfold county. *NGU Report 1998.021*, 11 pp. (in Norwegian).

Mogaard, J.O. (2001) Helicopter-borne geophysical measurements around Sandefjord, Vestfold county. *NGU Report 2001.003*, 12 pp. (in Norwegian).

Mogaard, J.O. and Beard, L.P. (2000) Helicopter-borne geophysical measurements around Skien, Telemark county. *NGU Report 2000.031*, 12 pp. (in Norwegian).

NRPA (2000) Radon in indoor air. Health risk, measurements and remedial measures. *StrålevernHefte*, **9** (revised edition), 24 pp., Østerås: Statens strålevern (in Norwegian).

Otton, J.K., Gundersen, L.C.S., Schumann, R.R., Reimer, G.M. and Duval, J.S. (1995) Uranium resource assessment and exploration data for geologic radon potential assessments in the United States. In *Application of Uranium Exploration Data and Techniques in Environmental Studies, IAEA Technical Document 827*, pp. 135–137.

Smethurst, M.A., Strand, T., Finne, T.E. and Sundal, A.V. (2006) Airborne gamma ray spectrometry and radon: Application of fixed-wing and helicopter surveying to the identification of radon affected areas—an analysis based on measurements over eastern Norway. *StrålevernRapport 2006:12*, 20 pp., Østerås: Statens strålevern (in Norwegian).

Smethurst, M.A., Strand, T., Sundal, A.V. and Rudjord, A.L. (submitted) A novel approach to radon-hazard mapping: Utilizing relationships between airborne gamma-ray spectrometer measurements and indoor radon concentrations. *Science of the Total Environment*.

Strand, T., Ånestad, K., Ruden, L., Ramberg, G.B., Jensen, C.L., Wiig, A.H. and Thommesen, G. (2001) Indoor radon survey in 114 municipalities. Short presentation of results, *StrålevernRapport 2001:6*, 14 pp., Østerås: Statens strålevern (in Norwegian).

Strand, T., Jensen, C.L., Ramberg, G.B., Ruden, L. and Ånestad, K. (2003) Mapping of radon concentration in 44 Norwegian municipalities. *StrålevernRapport 2003:9*, 10 pp., Østerås: Statens strålevern, (in Norwegian).

Stranden, E. (1986) Radon -222 in Norwegian dwellings. In *Proceedings of the symposium on radon and its decay products: occurrence, properties and health effects*. New York, US, 13–18 April 1986, *American Chemical Society Symposium Series*, **331**, 70–83.

Sundal, A.V., Henriksen, H., Soldal, T. and Strand., T. (2004) The influence of geological factors on indoor radon concentrations in Norway. *Science of the Total Environment*, **328**, 41–53.

Sundevall, S.E. (2003) Regional radon investigations, Kungälvs municipality. *Sveriges Geologiska Undersökning Report 2003:22* (in Swedish).